18TH WORLD CONFERENCE ON EARTHQUAKE ENGINEERING
WCEE2024
MILAN

MILAN, ITALY
30TH JUNE - 5TH JULY 2024

www.wcee2024.it

SIMULATION OF THE SEISMIC RESPONSE OF VERTICAL INSTRUMENTED ARRAYS IN LIQUEFIABLE SITES

R. Mohammadi[1], A. Chiaradonna[2] & P. Monaco[2]

[1] University of L'Aquila, Department of Civil, Construction-Architectural and Environmental Engineering, L'Aquila, Italy, rayka.mohammadi@student.univaq.it

[2] University of L'Aquila, Department of Civil, Construction-Architectural and Environmental Engineering, L'Aquila, Italy

Abstract: *The capability to correctly predict the liquefaction occurrence in numerical modelling has been largely assessed in many research groups and by adopting several constitutive models. However, less attention has been devoted to verifying the available approaches to simulate the soil behaviour from the small-strain range to the liquefaction attainment. In this context, earthquake records provided by vertical liquefaction arrays constitute a powerful tool to verify the goodness of constitutive models because data associated to earthquakes of different level of intensity are available and can be used to explore a wide range of shear strains in the prediction of the dynamic nonlinear soil behaviour.*
This study presents the simulation of two well-characterized liquefaction arrays, located in Japan and California (US), respectively. The numerical analyses have been carried out by adopting a critical state compatible, stress ratio-based, bounding surface plasticity constitutive model, in the last released version, implemented in a commercial finite difference platform. The model calibration is based on the results of site investigations, with special attention to cyclic and dynamic laboratory tests collected in previous studies and not often considered in the calibration of the most recent advanced constitutive models. The simulation results are compared with the records at the surface and those obtained through an equivalent liner method. This study enriches the discussion on the calibration of soil models and contribute to a step forward in improving the reproducibility of the nonlinear behaviour of soils from the small-strain range until failure and after liquefaction.

1. Introduction

Given the non-linear and irreversible nature of soil behaviour, properly predicting this latter, from small-strain conditions to liquefaction, is a challenging task, and requires accurate constitutive models and extensive validation. In the past, several researchers used instrumented reference sites, called liquefaction vertical arrays, to test the efficacy of computer codes and soil constitutive models (Elgamal et al. 1996; Cubrinovski et al. 1996; Ziotopoulou 2010). More recently, specific benchmarks aimed to validate nonlinear simulations by using ideal subsoil profiles and real test sites (Régnier et al. 2015, 2018; Khalil et al. 2021).

Among the several test sites, the vertical array close to the city of Sendai in Japan and the Wildlife Refuge Array in California (United States) are particularly interesting because well-investigated and equipped with sensors able to record real earthquakes.

The Sendai site was considered as validation case study in the framework of the PRENOLIN Project (Régnier et al. 2018), where the uncertainties associated with nonlinear simulations of 1D site effects during seismic events were evaluated. Sendai array was selected in the project because it underwent extensive site

characterization, including the measurements of shear wave velocity, V_s, compressional wave velocity, V_p, density profiles, and various laboratory tests on soil samples. The site selection criteria considered both strong and weak event recordings, plausibility of a 1D soil configuration, and the depth of the downhole sensor. Following this project, Tropeano et al. (2019) and Chiaradonna et al. (2019) used the same case of study for validating an innovative simplified pore water pressure model implemented in a nonlinear code for effective stress analyses.

The Wildlife Refuge Array in California (United States) is a quite old site which was largely investigated and simulated in the past. More recently, Ziotopoulou (2010) and Chen and Arduino (2021) used this case for the validation of the PM4Sand model (Boulanger and Ziotopoulou 2022) in the numerical computer codes FLAC (Itasca 2020) and Opensees, respectively.

In this paper, the two above mentioned instrumented sites: Sendai array in Japan and the Wildlife Liquefaction Array in California, are simulated by adopting the critical state compatible, stress ratio-based, bounding surface plasticity constitutive model, PM4Sand model (Boulanger and Ziotopoulou 2022), in the last released 3.2 version, implemented in the commercial finite difference code FLAC (Itasca 2020). The model calibration is based on the results of site investigations collected in previous studies, with special attention to cyclic and dynamic laboratory tests not often considered in the calibration of the most recent advanced constitutive models. For comparison, total stress analyses are also performed by using one of the most popular computer codes for seismic soil response: STRATA (Kottke et al. 2018), which adopts an equivalent linear approach in the frequency domain.

In the following Section 2, the Sendai site is firstly introduced, then the available soil investigations summarized and finally the performed simulations are described and discussed by comparing the recorded acceleration response spectra at the surface with the simulated ones. Similarly, Section 3 follows the same steps to describes the simulations carried out for the Wildlife site. The main findings of the study are finally summarized in the conclusions.

2. Sendai Site

Sendai is an array site from the PARI (2015) network in the North-East of Japan (Figure 1). The recording station consists of a surface accelerometer and a downhole sensor at 10.4 m depth, located near the Sendai port. The array is deployed in a Holocene sedimentary soil, called “beach ridge”, consisting of gravel and sand, formed through transportation and sedimentation by sea waves. This surface deposit is underlain by the Pliocene “Geba formation”, forming the Northern and Eastern hills and consisting of gravel stone, sandstone, tuff, tuffaceous siltstone, and lignite (OYO Corporation 2014). The site was chosen in the PRENOLIN Project for the 1D geometrical soil configuration, also checked with MASW measurements (Regnier et al. 2018). In the framework of the same project, an extensive investigation campaign was carried out to obtain the in-situ shear wave profile, using downhole PS logging; the stress-strain and strength properties were measured by laboratory tests on samples obtained on undisturbed sampling and recovered boring cores.

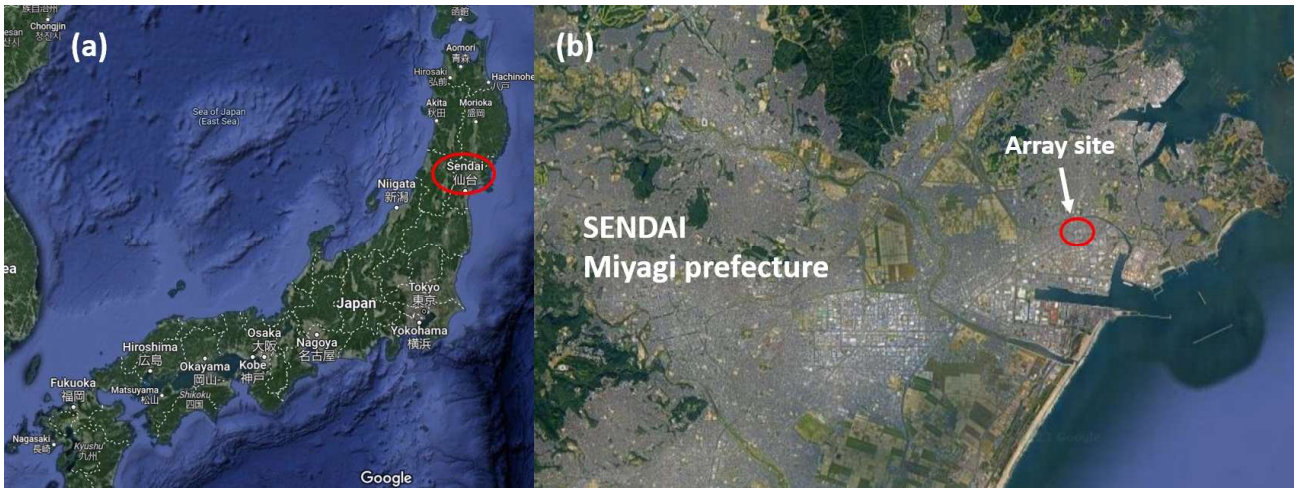

Figure 1. Sendai location in Japan (a) and close-up on Sendai and the array site (b)

As for the record motions, nine records of real seismic events were selected, representing three different Peak Ground Acceleration (PGA) levels (≥ 0.06, 0.02-0.03 g and ≤ 0.01 g) and approximately three distinct frequency contents at the downhole sensor. The numbering of input motion, from #1 to #9, corresponds to decreasing PGA amplitude (Regnier et al. 2018). The characteristics of the downhole and surface records are reported in Table 1. For simplicity, only the East-West (EW) components were considered in this study.

Table 1. EW components of the downhole and surface records

Record	Frequency content	Downhole PGA [g]	Surface PGA [g]
1	Low	0.251	0.405
4		0.025	0.075
8		0.005	0.009
2	Intermediate	0.063	0.223
5		0.026	0.052
9		0.004	0.010
3	High	0.062	0.183
6		0.035	0.074
7		0.012	0.033

2.1. Soil investigations available at Sendai site

Figure 2a shows the soil layering of the Sendai site. The upper part of the soil column is composed of loose gravel with a thickness of 1.25 m, overlying about 5 m of fine sand moderately dense sand with fine sand. In this layer, a 5 cm thick silty layer is detected, which contains organic silt and shell fractions. From 7.15 m in depth a slate, generally hard formation can be considered as the seismic bedrock. The ground water table is located at 1.45 m from the surface.

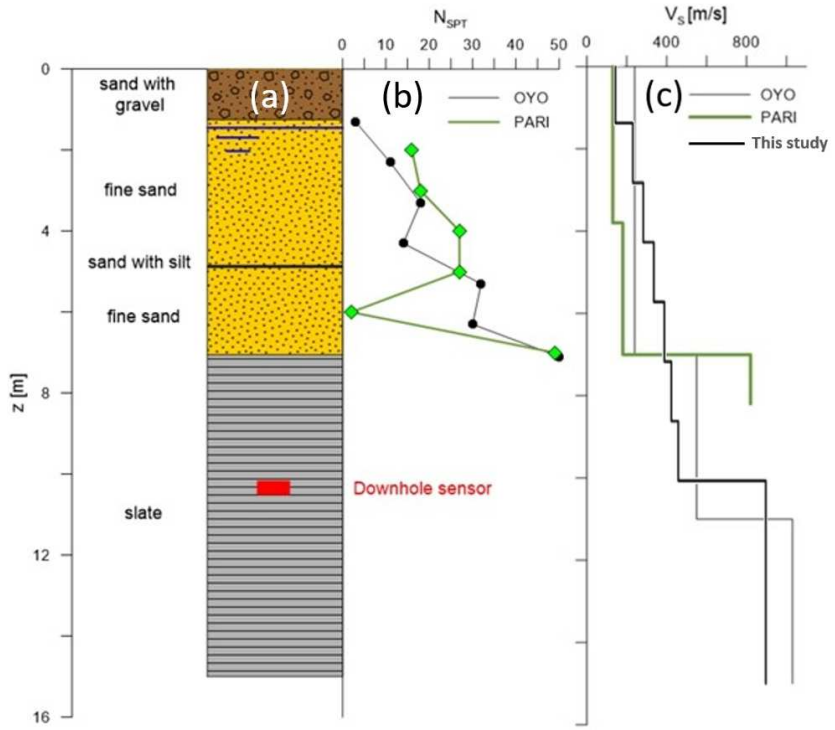

Figure 2. Soil layering (a), SPT (b) and V_s *(c) profiles of Sendai site*

Figure 2 also shows the number of blow counts obtained from a Standard Penetration Test - SPT (Fig. 2b) and the shear wave velocity, V_s, profiles as measured by OYO (2014) and reported by the PARI website (PARI 2015), as well as the adjustment of the shear wave velocity adopted in the PRENOLIN to obtain a better agreement with the surface/borehole transfer function empirically obtained (Regnier et al. 2018), also considered in this study. The results of the investigations performed by OYO Corporation show significant discrepancies from the data reported by PARI for both SPT blow count, N_{SPT}, and shear wave velocity profiles. N_{SPT} shows a reduction around 4.5 – 6 m, which is not present in the shear velocity profile. Main differences in the velocity profiles are observed in the shallowest four meters, where OYO reported a velocity of 240 m/s, which is almost two times the value of 130 m/s reported by PARI.

Undisturbed samples were retrieved at the depths of 3.3 and 5.4 m to conduct laboratory tests. Both samples were subjected to cyclic triaxial tests to determine deformation properties of soil, while a stress-controlled cyclic undrained triaxial test (CTX) and a consolidated-drained triaxial test (CID) were performed on the shallower sample. A cohesion *c'* = 1.2 kPa and an internal friction angle ϕ' = 43.6° were obtained from the CID test.

2.2. Geotechnical model of Sendai site used in the simulations

In the one-dimensional analyses carried out by means of FLAC and STRATA, a rigid bedrock was assumed at the depth of 10.4 m, where the downhole sensor is located. In FLAC, the soil column had a global width of 0.5 m and the grid consisted of 52 zones of 0.2 m each. While the downhole acceleration records were applied as input motions at the bottom of the column which was fixed both horizontally and vertically, the movement of the rest of the column was only restricted in the horizontal axis.

The shear wave velocity profile and the other soil properties are summarized in Table 2. For the calibration of the PM4Sand model of the liquefiable sandy sublayer, the three primary parameters: the apparent relative density (D_R), shear modulus coefficient (G_0), and the contraction rate parameter (h_{p0}) were defined (Table 2). The relative density was estimated through the correlation with the SPT as proposed by Idriss and Boulanger (2008). The parameter G_0 rules the small-strain shear modulus and was inferred from the in-situ V_s measurements. The h_{p0} parameter is the last to determine by achieving the cyclic resistance curve that is as close as possible to that of the fine sand as experimentally defined with CTX tests (Fig. 3b), and it is calibrated after fixing the two other parameters.

After the PM4Sand parameters has been calibrated for each layer, the shear modulus reduction and damping ratio curves have been simulated. Figure 3a reports the comparison between the experimental curves and that reproduced in FLAC through a simulated cyclic laboratory test at the depth of 3.5 m.

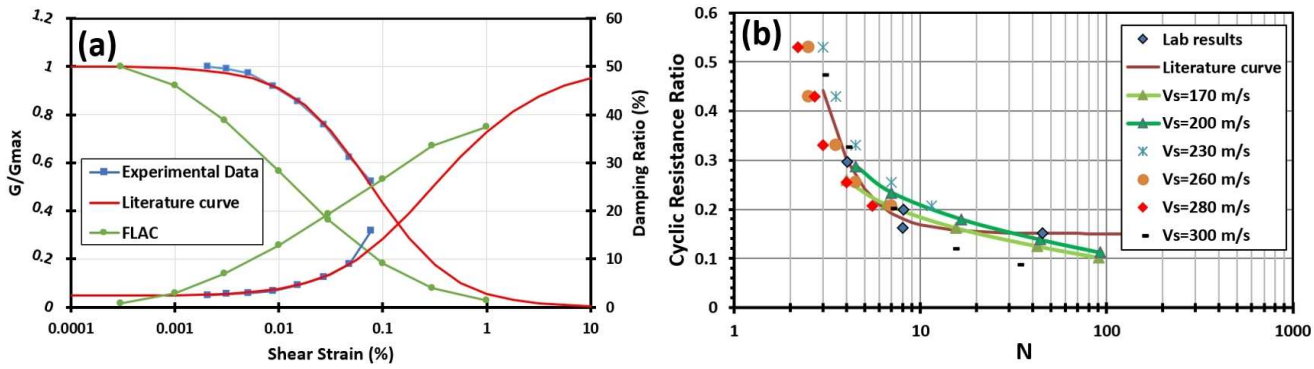

Figure 3. Experimental and simulated (a) normalized shear modulus reduction and damping ratio curves; (b) cyclic resistance curves for the different V_s layers

Concerning the non-liquefiable layers of the soil column, a simple elastic isotropic model in combination with an hysteretic damping was adopted. The elastic isotropic model requires the soil density, the elastic shear

modulus G_{max} (inferred from the V_s measures) and the elastic bulk modulus K (calculated for a Poisson ratio equal to 0.3 according to the elasticity theory), as reported in Table 2.

The hysteretic damping reproduces the shear modulus reduction curves, G/G_{max}, which are selected from a range of published literature curves suited to different materials and parameters, which are experimental data from Regnier et al. (2016). The hysteretic damping is introduced in the simulation according to the sigmoidal (sig4) model, available in FLAC, which is defined as follows:

$$G = y_0 + \frac{a}{1+\exp(-\frac{L-x_0}{b})} \quad (1)$$

where G is the secant modulus such that $\bar{\tau} = G.\gamma$ and $L = \log_{10}(\gamma)$, and a, b, x_0 and y_0 are the model parameters to be defined. These latter have been defined with a regression analysis and are reported in Table 2. No hysteresis damping was assigned to the slate layer since it is modelled as a visco-elastic rock. Finally, to introduce in the analyses the dissipative properties of the soils also in the elastic strain range, a viscous Rayleigh damping of 1% was applied at the natural frequency of the modelled soil column (f=6.173 Hz) to the whole profile.

In the dynamic analyses performed with STRATA, the same soil parameters and shear modulus and damping ratio curves used in the FLAC model are also considered.

Table 2. Soil properties and PM4Sand parameters used in the analyses for the Sendai case.

Depth [m]	**Soil type**	**Unit weight, γ [kN/m³]**	**V_s [m/s]**	**N_{SPT}**	**PM4Sand parameters**			**Sig4 Model Parameters**			
					D_R	**G_0**	**h_{p0}**	***a***	***b***	**x_0**	**y_0**
0 – 1.0	Sand with gravel	18.15	120	-	-			0.999	-0.3899	-1.1052	0.00022
1.0 – 1.45	Fine sand	18.15	170	16	-			0.999	-0.3747	-0.9835	0.000204
1.45 – 2.0			170	16	0.590	1180.65	0.42	-			
2.0 – 3.0			200	18	0.625	1433.20	0.41	-			
3.0 – 4.0		18.54	230	27	0.766	1745.23	0.04	-			
4.0 – 5.0			260	27	0.766	2046.64	0.025	-			
5.0 – 6.0			280	2	0.208	2181.15	0.38	-			
6.0 – 7.0			300	49	1.032	2352.00	0.13	-			
7.0 – 8.0	Slate (rock)	24.33	550	-	-			-			
8.0 – 10.4		24.33	550								

2.3. Simulation results

Simulations were performed for the selected input motions (Table 1) and the results are expressed in terms of comparison between recorded and simulated acceleration response spectra at the surface. To achieve uniformity of the representation scale, the spectral accelerations were normalized with respect to the PGA recorded at the surface for each input motion. Figure 4 shows the results of the simulations for the low, intermediate, and high frequency content input motions, respectively from left to right.

It is possible to observe that for low intensity motions, both nonlinear (FLAC) and equivalent linear (STRATA) analyses provided a good agreement with the response at the surface (see inputs #7 to #9). This is due to the fact that the soils are behaving elastically in the small-strain range and the elastic properties are the same in both numerical models.

As soon as the intensity of the shaking increases, the nonlinear soil behavior is becoming a predominant factor in the soil response at the surface and, in this case, only the effective stress analyses performed in FLAC are able to track the increase of the predominant period and the deamplification of the motions (see inputs #1 to #3). Indeed, large discrepancies between simulations and records can be observed in the case of the STRATA analyses in terms of both maximum spectral acceleration and predominant periods (see inputs #1, #3 and #5).

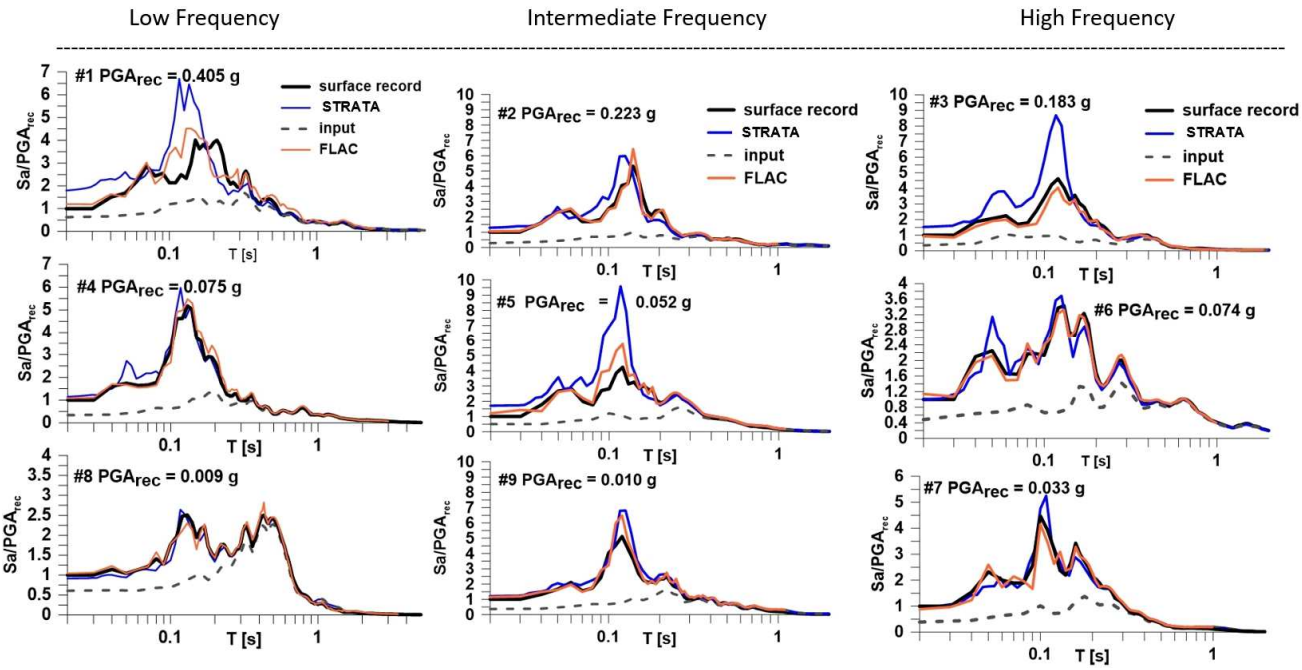

Figure 4. Comparison for the different frequency ranges of input motions between recorded and simulated acceleration response spectra at the surface performed with STRATA and FLAC

3. Wildlife Site

The Wildlife Liquefaction Array (WLA) is located in the floodplain of the Alamo River, in the Imperial Valley, 160 km East of San Diego, California (Fig. 5a). In this area, liquefaction evidence was observed during the 1930, 1950, 1957, 1981 and 1987 earthquakes. Because of the high seismicity of this region, USGS (United States Geological Survey) decided to install accelerograms and piezometers in 1982.

Due to the plain topographic condition and the horizontal layered deposits (Figure 5b), Wildlife constitutes a natural laboratory for monitoring seismic site response. The site was equipped with surface and downhole accelerometers and six electrical probe piezometers. The downhole sensor was placed at a depth of 7.5 m, immediately below the liquefiable layer, and five of the six piezometers were placed within the liquefiable layer.

Figure 5. Location of Wildlife Liquefaction array in the Imperial Valley, California (a) and satellite image of the array site (b)

The Wildlife Liquefaction Array was triggered four times during the Superstition Hills earthquake sequence of 23 and 24 November 1987 (Table 3): the Elmore Ranch earthquake, a 6.2 moment magnitude event occurred on November 23rd, 1987, and the Superstition Hills earthquake, a Mw = 6.6 event that occurred on the next day.

Table 3. Seismic sequence of the 1987 earthquakes (Zeghal and Elgamal 1994)

Event	Date (1987)	Time (PST)	Magnitude	Epicentral distance [km]	Peak horizontal surface acceleration [g]
Elmore Ranch	November 23	17:54	MW 6.2	23	0.13
(aftershock)	November 23	22:23	ML 4.0	-	0.01
Superstition Hills	November 24	05:15	MW 6.6	31	0.21
(aftershock)	November 24	05:34	ML 4.8	-	0.02

During Elmore Ranch earthquake, the shaking level was relatively low, so that no seismic excess pore pressure was recorded, while Superstition Hills event caused full liquefaction (Thilakaratne and Vucetic 1990). Sand boils erupted water and muddy sediment, and turned the arid array site into a quagmire, affecting an area of about 33 ha in the floodplain. Liquefaction interested the silty sand layer, especially in the upper part of the stratum (WSA) as reported by Vucetic and Dobry (1986). Extensive ground cracking, indicating lateral spreading, accompanied liquefaction at the array site; the cumulative opening across ground cracks was 126 mm (Holzer et al. 1989).

3.1. Soil investigations available at Wildlife site

The soil profile can be subdivided into four main soil layers (Fig. 6 from Chiaradonna (2016)). The upper 2.5 m consists of sandy silt, silt and clayey silt, which was recognized as a flood-plain deposit; cone penetration test data indicate that such sediments are very loose and soft. A silty sand layer, which is understood to be the liquefiable layer in the profile, extends for 4.3 m below. This deposit contains two sub-units identified as Wildlife sand *A* and *B* (WSA and WSB), respectively; the first 1 m consists of very loose to loose sandy silt, while the second sub-unit consists of loose to medium silty sand to very fine sand. The contact between the two sub-units is gradual. The second layer was interpreted to be a point-bar deposit, because located on the

concave side of the river meander curve. A lacustrine silty clay deposit extends from 6.8 to 12 m depth, underlain by a cemented silt (Bennett et al. 1984).

The ground water table has been assumed at 1.45 m depth as reported by Holzer and Youd (2007). The Vs profile assumed in the study (in black) is directly based on the Cross-Hole test data (in blue) reported by Vucetic and Dobry (1986) and it is more detailed than the profile proposed by Holzer and Youd (2007). The SPT blow counts profile also highlights the differences between WSA and WSB layers

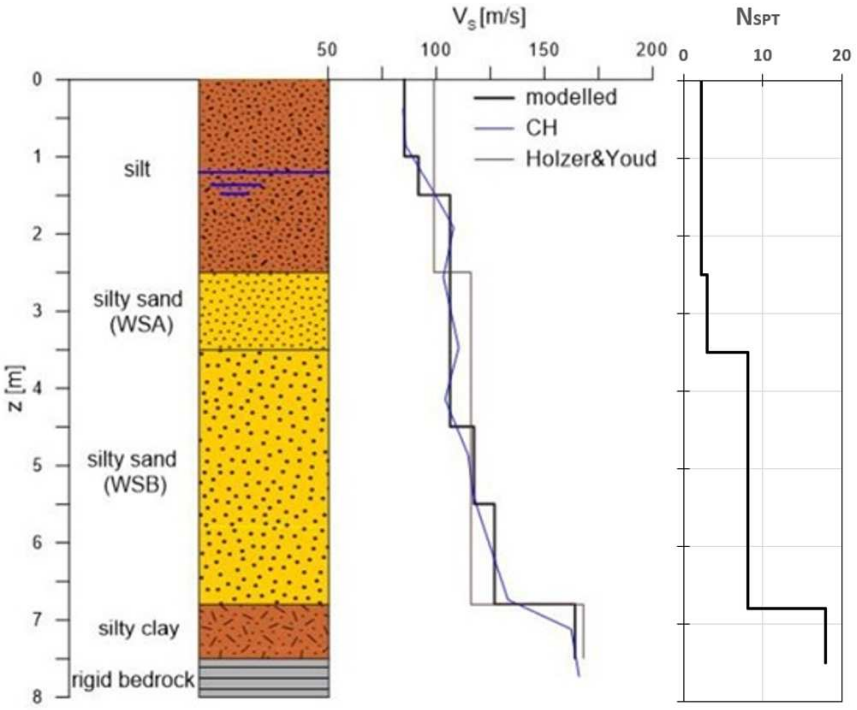

Figure 6. Soil column (a), shear wave velocity profiles (b), and SPT blow count profile (c)

3.2. Geotechnical model of Wildlife site used in the simulations

In the FLAC model, the entire soil column was modelled to be 0.5 m wide with rectangular grid of 16 zones of thicknesses ranging between 0.2 and 0.5 m. Similarly to the boundary conditions adopted for the Sendai case, the movement of all nodes were limited in the x-direction and the displacement of the base of the column was restricted in both directions.

For the calibration of the PM4Sand model of the liquefiable sandy sublayer (WSA and WSB), the three primary parameters: the apparent relative density (D_R), shear modulus coefficient (G_0), and the contraction rate parameter (h_{p0}) were defined (Table 4). The relative density was estimated through the correlation with the SPT as proposed by Idriss and Boulanger (2008). The parameter G_0 rules the small-strain shear behaviour and was defined based on the in-situ V_s measurements. The h_{p0} parameter is the last to determine by achieving the cyclic resistance curve that is as close as possible to that of the fine sand as experimentally defined by Vucetic (1986) for the two sublayers (Fig. 7b), and it is calibrated after fixing the two other parameters.

After the PM4Sand parameters has been calibrated for each layer, the shear modulus reduction and damping ratio curves have been simulated. Figure 7a reported the comparison between the experimental curves reported by Vucetic (1986) and that reproduced in FLAC through the simulation of cyclic laboratory tests.

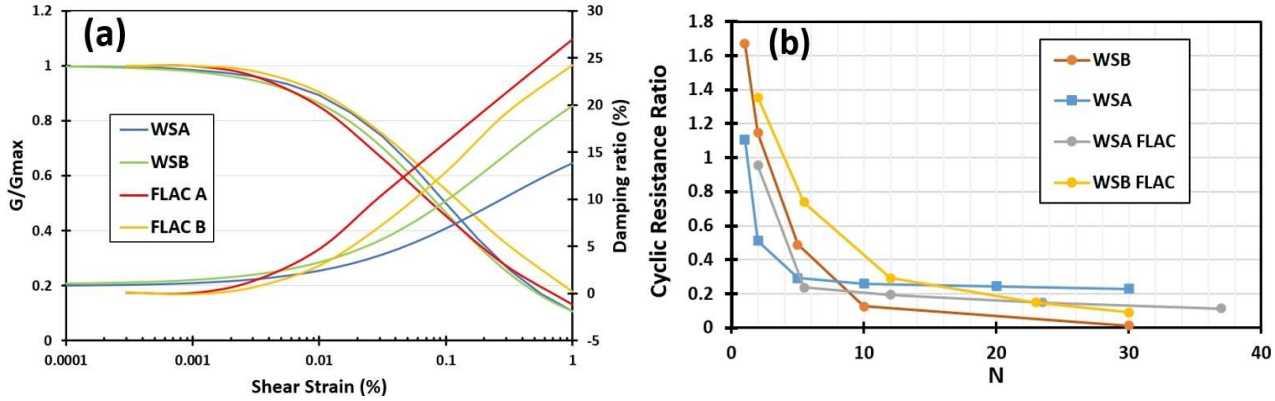

Figure 7. Experimental and simulated (a) normalized shear modulus and damping ratio curves, and (b) cyclic resistance curves

Table 4. Soil properties and PM4Sand parameters used in the analyses for the Wildlife case.

Depth [m]	Soil type [damping curve]	Unit weight, γ [kN/m^3]	V_s [m/s]	N_{SPT}	PM4Sand parameters			Sig4 Model Parameters			
					D_R	G_0	h_{p0}	a	b	x_0	y_0
0 – 1.0	Silt [Vucetic – Dobry (1991) PI=15]	18.65	85.31	2.2	-			1	-0.545	-1.216	0
1.0 – 1.5			91.81								
1.5 – 2.5			106.39								
2.5 – 3.5	Silty Sand (WSA)	18.82	106.39	3	0.38	350	1.9	-			
3.5 – 4.5	Silty Sand (WSB)		106.39	8.2	58	266	0.86	-			
4.5 – 5.5			117.49								
5.5 – 6.8			126.92								
6.8 – 7.5	Silty Clay [Vucetic – Dobry (1991) PI=30]	19.18	164.14	18	-			1	-0.563	0.889	0

As for the previous case, a universal Rayleigh damping of 1% was applied to the entire column structure at its natural frequency of 2.656 Hz. Meanwhile, the sublayers were given sigmoidal (sig4) hysteresis damping, and the specific parameters can be found in Table 4.

3.3. Simulations results

Simulations were performed for both components of the Elmore Ranch and Superstition Hills earthquakes. The results are expressed in terms of comparison between recorded and simulated acceleration response spectra at the surface. Regarding the Elmore Ranch earthquake which did not induce liquefaction in the Wildlife Refuge Array, the obtained results are reported in Figure 8. Both codes are able to reproduce the recorded PGA at the surface where there is a certain range of periods (0.09 – 0.5s) for which a misprediction can be observed. This is mainly due to the uncertainties related to the geotechnical model definition.

For the Superstition Hills earthquake which was a stronger event and has caused liquefaction in the Wildlife Refuge Array, the obtained results are reported in Figure 9. Also in this second case, the uncertainties can be still observed in the same period range. However, especially for the NS component, the simulation performed in FLAC with the advanced soil constitutive model is largely better in terms of maximum spectral acceleration than that obtained with STRATA.

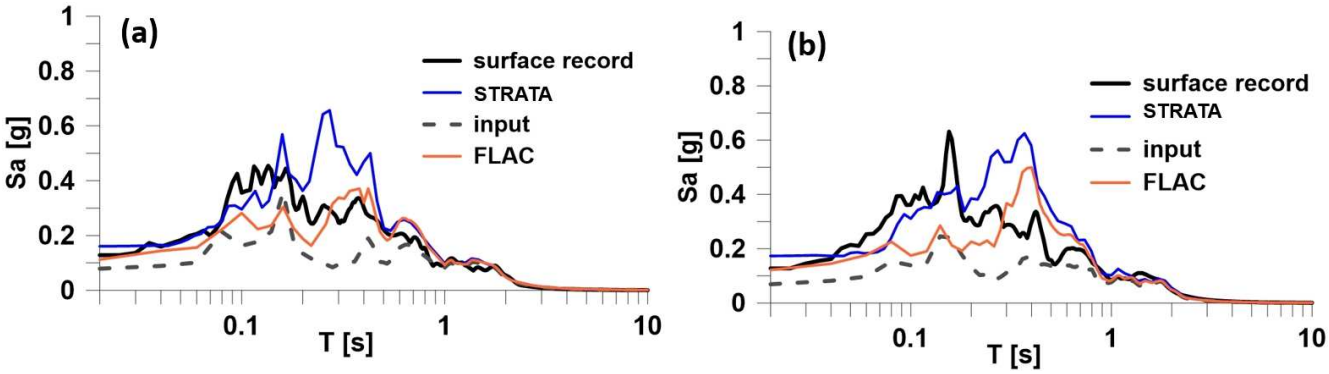

Figure 8. Comparison among simulated and recorded acceleration response spectra for the EW (a) and NS (b) components of the Elmore Ranch event.

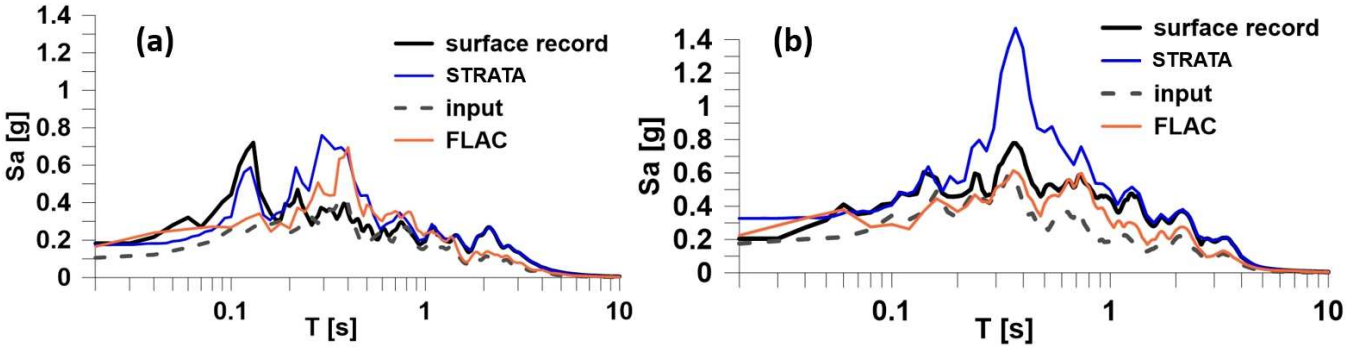

Figure 9. Comparison among simulated and recorded acceleration response spectra for the EW (a) and NS (b) components of the Superstition Hills event.

4. Conclusions

This paper presented total and effective stress numerical simulations of two real-life sites of Sendai and Wildlife Liquefaction Array using STRATA and FLAC.

As expected, the effective stress analyses (FLAC) yield results that are closer to the experimental records in comparison to the total stress analysis (STRATA). This is mainly due to consideration of the excess pore water pressure which has direct affect in the behaviour of the soil.

Future possible investigations may include comparing the achieved results with the simulations of other codes and performing similar total stress analyses on FLAC to verify the extent to which the outcomes vary from those of STRATA or from the introduced FLAC effective stress analyses.

5. References

Bennett M.J., McLaughlin P.V., Sarmiento J.S., Youd T.L. (1984). *Geotechnical investigation of liquefaction sites, Imperial Valley, California*, US Geological survey, Menlo Park, California, USA.

Boulanger R. W., Ziotopoulou K. (2022). PM4Sand (Version 3.2): A sand plasticity model for earthquake engineering applications, Report No. UCD/CGM-22/02, Center for Geotechnical Modeling, University of California, Davis, CA, March, 112 pp.

Chiaradonna A. (2016). *Development and Assessment of a Numerical Model for Non-Linear Coupled Analysis on Seismic Response of Liquefiable Soils*, PhD Thesis in Geotechnical Engineering, March 2016.

Chiaradonna A., d'Onofrio A., Silvestri F., Tropeano G. (2019). Prediction of non-linear soil behaviour in saturated sand: A loosely coupled approach for 1d effective stress analysis, In *Earthquake Geotechnical Engineering for Protection and Development of Environment and Constructions*, pp. 1746-1753.

Chen L., Arduino P. (2021). *Implementation, Verification, and Validation of the PM4Sand Model in OpenSees*, PEER Report No. 2021/02, Pacific Earthquake Engineering Research Center, University of California, Berkeley, Department of Civil and Environmental Engineering, University of Washington, March 2021.

Cubrinovski M., Ishihara K., Tanizawa F. (1996). Numerical simulation of the Kobe Port Island liquefaction. In *Proc. 11th World Conf. Earthquake Engineering* (Vol. 330). Acapulco, Mexico: Elsevier Science Ltd.

Elgamal A.W., Zeghal M., Parra E. (1996). Liquefaction of reclaimed island in Kobe, Japan, *Journal of Geotechnical Engineering*, 122(1): 39-49.

OYO Corporation (2014). *Report of soil investigation: Sendai District and Onahama District*, Report from the PreNoLin Project, Nice, France.

Holzer T.L., Youd T.L. (2007*).* Liquefaction, ground oscillation and soil deformation at the Wildlife array, California, *Bulletin of the Seismological Society of America*, 97(3): 961-976.

Holzer T.L., Youd T.L., Hanks T.C. (1989). Dynamics of liquefaction during the 1987 Superstition Hills, California, earthquake. *Science*, 244: 56-69.

Idriss I.M., Boulanger R.W. (2008). *Soil Liquefaction during Earthquakes*, Earthquake Engineering Research Institute, Monograph Series, 19.

Itasca (2020). *FLAC – Fast Lagrangian Analysis of Continua*, Version 8.1, Minneapolis, MN: Itasca Consulting Group, Inc.

Khalil C., Regnier J., Lopez-Caballero F., Alves-Fernandes V., Chiaradonna, A. et al. (2022). LICORNE a benchmark on numerical method for non-linear site response analysis involving pore water pressure. *Proc. 3rd European Conf. on Earth. Eng. & Seismology*, 3ECEES, Bucharest.

Kottke A.R., Wang X., Rathje E.M. (2018). *Strata Technical Manual*, Retrieved from https://github.com/arkottke/strata/blob/master/manual/manual.pdf

PARI (2015). *http://www.eq.pari.go.jp/kyosin/data/pnt/sendai-g.htm*

Régnier J., Bonilla L.F., Bard P.Y., Bertrand E., Hollender F., Kawase H., Watanabe K. (2016). International benchmark on numerical simulations for 1D, nonlinear site response (PRENOLIN): Verification phase based on canonical cases, *Bulletin of the Seismological Society of America*, 106(5): 2112-2135.

Régnier J., Bonilla L.F., Bard P.Y., Bertrand E., Hollender F., Kawase H., ..., Verrucci, L. (2018). PRENOLIN: International benchmark on 1D nonlinear site-response analysis − Validation phase exercise, *Bulletin of the Seismological Society of America*, 108(2): 876-900.

Thilakaratne V., Vucetic M. (1990). Analysis of the seismic response at the Imperial Wildlife Liquefaction Array in 1987, *Proceedings of Fourth US National Conference on Earthquake Engineering*, May 1990, Palm Springs, California, vol. 3.

Tropeano G., Chiaradonna A., d'Onofrio A., Silvestri F. (2019). A numerical model for non-linear coupled analysis of the seismic response of liquefiable soils, *Computers and Geotechnics*, 105: 211-227.

Vucetic M. (1986). *Pore pressure buildup and liquefaction at level sandy sites during earthquakes*, PhD Dissertation, Rensselaer Polytechnic Institute, Troy, NY, USA.

Vucetic M., Dobry R. (1991). Effect of soil plasticity on cyclic response, *Journal of Geotechnical Engineering*, 117(1): 89-117.

Zeghal M., Elgamal A.W. (1994). Analysis of site liquefaction using earthquake records, *Journal of Geotechnical Engineering*, 120: 996-1017.

Ziotopoulou K. (2010*). Evaluating model uncertainty against strong motion records at liquefiable sites*, Master of Science in Civil and Environmental Engineering, University of California, Davis, USA.